Epoxy–Nanocomposites with Ceramic Reinforcement for Electrical Insulation

E. Amendola,[1,2] A. M. Scamardella,[1,3] C. Petrarca,[4] D. Acierno[3]

[1]*Institute of Composite and Biomedical Materials, Italy's National Council of Research, Piazzale Enrico Fermi (P.le E. Fermi) 1, 80055 Portici, Naples, Italy*
[2]*Technological District of Polymer and Composite Materials Engineering and Structures, IMAST, Piazzale Enrico Fermi (P.le E. Fermi) 1, 80055 Portici, Naples, Italy*
[3]*Department of Materials and Production Engineering, University of Naples "Federico II," Piazzale Tecchio (P.le Tecchio) 80, 80125 Naples, Italy*
[4]*Department of Electrical Engineering, University of Naples "Federico II," via Claudio 21, 80125 Naples, Italy*

Received 28 April 2011; accepted 28 April 2011
DOI 10.1002/app.34782
Published online 11 August 2011 in Wiley Online Library (wileyonlinelibrary.com).

ABSTRACT: Ceramic nanoparticles, that is, SiO_2, TiO_2, and Al_2O_3 nanoparticles, with increasingly high thermal conductivity (λ), represent good candidates for improving the thermophysical properties of epoxy resins. In this study, the influence of filler addition on the thermal, mechanical, and dielectric properties were investigated by means of differential scanning calorimetry, dynamic mechanical analysis, and dielectric spectroscopy to measure λ, storage and loss moduli, dielectric permittivity, and volume resistivity. Moreover, morphological investigations by scanning electron microscopy were performed to confirm the particle dispersion into the epoxy matrix. The results show that both the elastic modulus and glass-transition temperature increased with particle content. An enhancement of λ was also observed at high filler contents because of the formation of heat conductive pathways within the matrix. The nanocomposites' relative permittivity at 50 Hz was lower, whereas the dielectric loss was slightly higher compared with that of the neat epoxy matrix. A decrease in the relative permittivity with increasing frequency, both for the unfilled epoxy resin and epoxy–nanocomposites, was observed. J Appl Polym Sci 122: 3686–3693, 2011

Key words: dielectric properties; resins; thermal properties

INTRODUCTION

Epoxy resins are widely used for industrial applications, such as structural composites, adhesives, surface coatings, and insulation in high-voltage apparatuses, rotating machines, and transformers. The insulation of rotating machines is subjected to multiple and concomitant stresses, for example, electrical, mechanical, and thermal stresses.[1] The heat generated during operations might potentially affect the structural integrity of the final product, if it is not dissipated. Thus, the improvement of heat dissipation in electrical and electronic devices has recently become a very important issue. Although thermoset resins exhibit quite low thermal conductivities (λ),[2] they are frequently used as electrical insulating materials.

It is well known[3] that the inclusion of solid particles, such as ceramics or metals, improves λ of the resulting composites. The filler content and its average shape and dimensions affect the resulting material properties, but on the other hand, the addition of a high filler content can deteriorate the processability and electrical performance of insulating material.

The use of nanosized particles has been proposed in the recent scientific literature as an alternative to conventional fillers. When the enormous specific surface area is taken advantage of, strong improvements are noticed as a result of nanoparticle inclusion in polymeric matrices. It has been anticipated[4] that the combination of nanoparticles with traditional resin systems may result in the preparation of nanocomposites with enhanced electrical, thermal, and mechanical properties.

In recent years, epoxy-based nanocomposites have been increasingly studied, and many research groups have published interesting articles about the properties of such materials. Generally, the results are limited to a single or double issue (either mechanical or thermal or electrical): Singha and Thomas[5] investigated the dielectric properties of epoxy–nanocomposites with insulating nanofillers [alumina (Al_2O_3), titanium dioxide (TiO_2), and ZnO] at low filler contents. Morshuis et al. published results on the λ[6] and dielectric properties[7] of three different epoxy-based composites containing silica

Correspondence to: E. Amendola (amendola@unina.it).

TABLE I
Properties of the Inorganic Nanoparticles Used for the Epoxy–Nanocomposites

Nanoparticles	Average size (nm)	Surface area (m^2/g)	Shape	λ (W/mK)
Al_2O_3	40–47	35–43	Spherical	40
SiO_2	12	200	Spherical	1.4
TiO_2	21	50–70	Spherical	11

(SiO_2), Al_2O_3, and aluminum nitride nanofillers. Gupta et al.[8] measured the complex permittivity and reported results on the dynamic mechanical analysis (DMA) of epoxy–Al_2O_3 nanocomposites.

To overcome the limitations of the previous works, in this study, we prepared epoxy composites containing SiO_2, TiO_2, and Al_2O_3 nanofillers at different weight percentages and characterized their thermal and dielectric properties; these tests were supported by a morphological analysis of the test samples.

EXPERIMENTAL

Materials

The epoxy resin was supplied by Elantas Camattini S.p.a. (Parma, Italy) A diglicydyl ether of bisphenol A epoxy resin (DGEBA), with an epoxide equivalent of 187 g/equiv, was cured with 90 phr methyl tetrahydrophthalic anhydride (MTHPA) as a hardener. The addition of 0.25 phr methyl imidazole was used as a catalyst for the crosslinking reaction. Al_2O_3 (supplied by Sigma Aldrich), SiO_2 (Aerosil 200 by Degussa) and TiO_2 nanoparticles (Aeroxide P25 by Degussa) were used for composite preparation (see Table I). The amounts of ceramic particles added were 1, 3, 5, and 7 wt % with respect to the total mass of the epoxy system (i.e., epoxy plus curing agent).

Characterization techniques

A scanning electron microscope (FEI Quanta type 200F, Hillsboro, OR) was used to analyze the inorganic filler dispersion morphology. Cryogenically fractured surfaces of the samples were gold-coated before scanning electron microscopy (SEM) studies to avoid electrostatic charging and were examined at a 20–30-kV accelerating voltage.

The thermal stability of the samples was investigated by thermogravimetric analysis (TGA) with a TA Instruments Q-5000 balance at a heating rate of 10°C/min up to 700°C in a nitrogen atmosphere.

The λ values of the neat epoxy resin and nanocomposites were estimated by modulated differential scanning calorimetry (MDSC) with a TA Instruments Q-1000 DSC (New Caste DE), according to ASTM E 1952. The conductivity value was derived from measurements of the heat capacity and apparent heat capacity of two samples of different geometry: cylinders 6.3 mm in diameter and 0.4 and 3.5 mm thick, respectively. The specific heat capacity of the thin sample, embedded in a nonhermetic pan, was measured by MDSC with a quasi-isothermal method with the following experimental parameters: equilibration at 30°C, modulation amplitude of ±0.5°C, and period of 80 s, to ensure that the thermal equilibrium across the sample was reached. The apparent heat capacity of the thick sample was measured with a thin aluminum disk as a reference and a sample holder. Tiny drops of silicon oil were used to decrease the thermal resistance at the interfaces. MDSC was run with the same experimental parameter used for the specific heat capacity measurement. DMA was carried out by a TA Instruments DMA Q800 at a heating rate of 5°C/min in a range of temperatures from 0 to 200°C. A single-cantilever geometry was adopted with a deformation amplitude of 15 μm at a frequency of 1 Hz.

Electrical characterization was performed by evaluation of the direct-current (dc) volume resistivity (ρ_v), relative dielectric permittivity (ε_r), and dissipation factor (tg δ) at a high voltage and 50 Hz and, at last, the frequency spectra in the frequency range 10^2–10^6.

Nanocomposite preparation

Nanocomposites containing 1 and 3 wt % Al_2O_3, SiO_2, and titania nanoparticles were prepared to investigate the effect of the ceramic filler content and composition on the thermomechanical behavior of the epoxy resin. Moreover, to improve λ of the epoxy-based composites, Al_2O_3 was selected because of its high λ (40 W/mK).

The higher Al_2O_3 content used in this investigation was 30 wt %. The addition of a higher filler amount is strongly detrimental to processing and results in a remarkable viscosity increase. For this reason, the aforementioned composition was fixed as a limiting value, even tough. Kim et al.[9] reported the achievement of a percolative pathway for spherical monodispersed particles in the range between 40 and 70 vol %, which corresponded to 70 and 90 wt % in the case of epoxy and Al_2O_3.

Combined dispersion techniques were used for nanocomposite preparation, namely, mechanical mixing and sonication.[10] Before use, all of the nanoparticles were dried at 80°C overnight *in vacuo*. A suitable amount of nanoparticles was added to the DGEBA component of the epoxy system before curing. The dispersion was mechanically mixed with a high-speed homogenizer (Turrax T25, Staufen, Germany) at 6500 rpm for 10 min and subsequently sonicated with an ultrasonic processor (Hielscher UP200S, Teltow, Germany) at 50% of the maximum

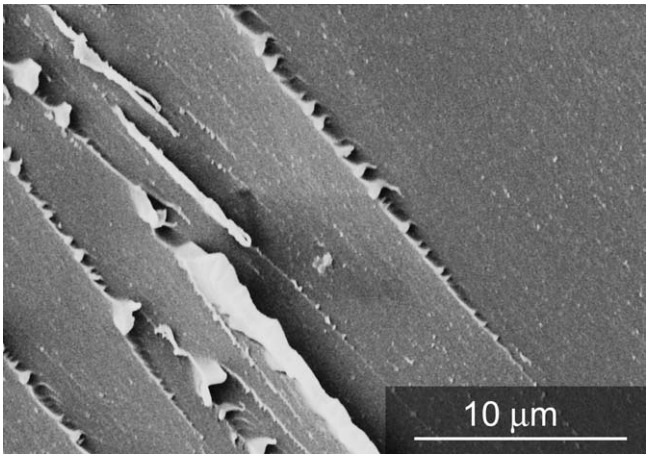

Figure 1 SEM micrograph of the fractured surface of the neat epoxy resin.

amplitude (200 W) for about 30 min. After the addition of MTHPA hardener (90 phr), the system was further mixed with a planetary vacuum mixer (Thinky). The nanocomposite samples were cured according to the technical data sheet of the epoxy resin (4 h at 80°C, 3 h at 100°C, and 4 h at 140°C).

RESULTS AND DISCUSSION

Morphology and dispersion

SEM analysis was carried out on the fracture surface of the neat epoxy resin and its composites to qualitatively evaluate the particle–matrix interface and to reveal the presence of undesired particle aggregations. In Figure 1, brittle behavior can be observed for the neat epoxy, which was characterized by a large smooth area and fracture steps in the crack propagation.

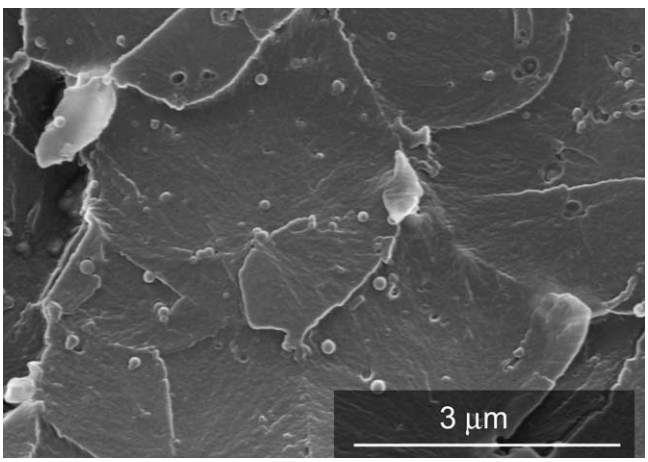

Figure 2 SEM micrograph of the fractured surface of the epoxy–nanocomposite containing 3 wt % Al_2O_3.

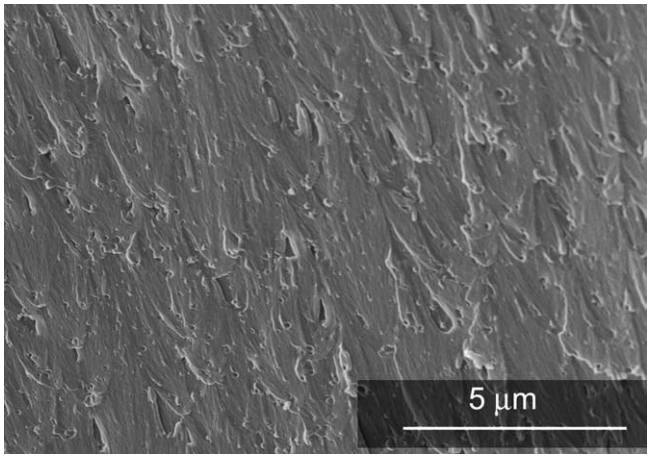

Figure 3 SEM micrograph of the fractured surface of the epoxy–nanocomposite containing 5 wt % Al_2O_3.

The epoxy–nanocomposites containing Al_2O_3 particles were selected as the most representative samples because of the higher λ exhibited by the selected filler. The fracture surfaces of the Al_2O_3–epoxy–nanocomposites at 3, 5, and 30 wt % are shown in Figures 2–4, respectively.

Rough and deformed fracture surfaces were observed for the Al_2O_3 nanocomposites. In particular, in Figure 2, single particles can be identified with an average diameter of about 60–70 nm, closely related with nominal particles' dimension. Careful observations performed on samples containing 3, 5, and 30 wt % Al_2O_3 (Figs. 2–4) evidenced a good and homogeneous dispersion of particles without clustering and aggregates.

Figures 5 and 6 show the fractured surface morphology of the TiO_2 and SiO_2 nanocomposites, respectively, at 3 wt %. The absence of particle aggregates and a surface significantly rougher than the neat epoxy resin (see Fig. 1) were observed for the TiO_2 and SiO_2 nanocomposites.

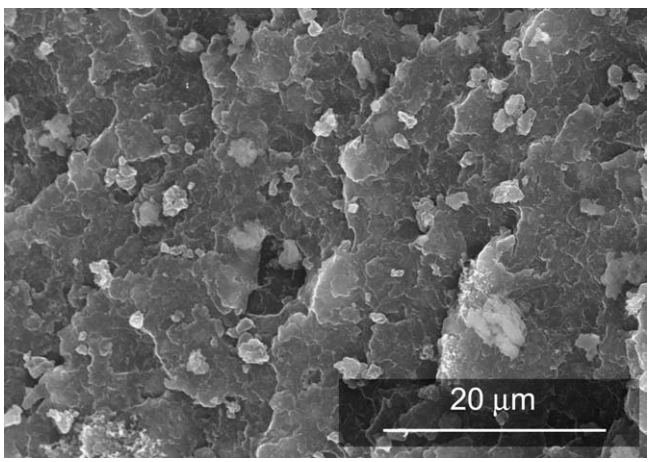

Figure 4 SEM micrograph of the fractured surface of the epoxy–nanocomposite containing 30 wt % Al_2O_3.

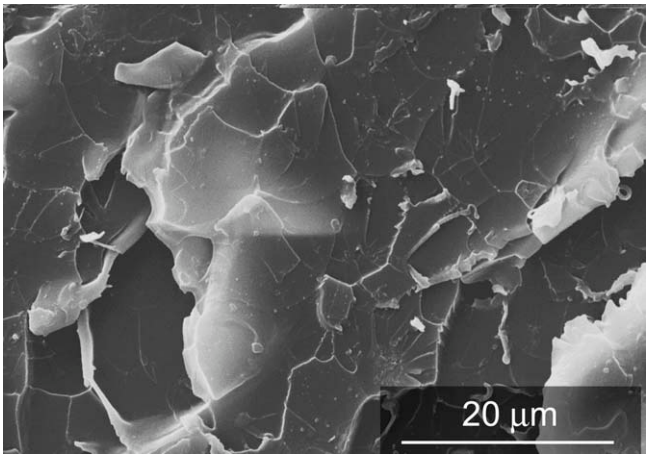

Figure 5 SEM micrograph of the fractured surface of the epoxy–nanocomposite containing 3 wt % TiO_2.

Thermal stability of the nanocomposites

Figure 7 shows the TGA results of the Al_2O_3–epoxy–nanocomposites in a temperature range between 40 and 600°C. The initial thermal decomposition temperatures (T_{id}) evaluated at 3% weight loss are reported in Table II for all of the composites.

The nature and amount of nanoparticles dispersed into the epoxy matrix affected the degradation phenomena. Nevertheless, no definite trend was evident with filler loading.

Dynamic mechanical properties

DMA was used to evaluate the effects of solid fillers on the dynamic mechanical properties of the epoxy system.

Storage modulus (E') and damping factor (tan δ) curves of neat epoxy and its Al_2O_3 nanocomposites are shown in Figures 8 and 9. The addition of ceramic particles determined an increase in the elastic

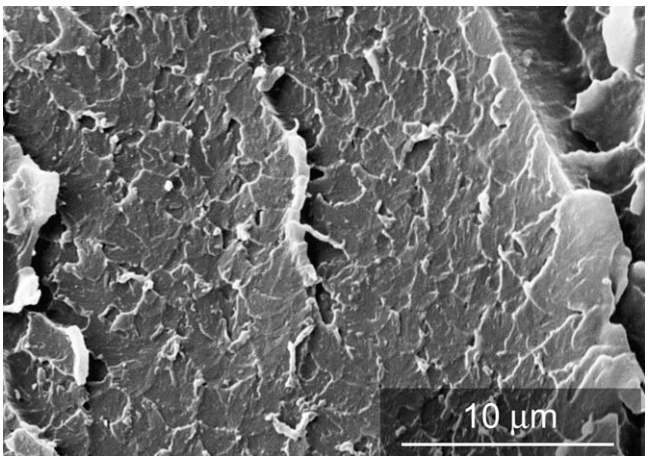

Figure 6 SEM micrograph of the fractured surface of the epoxy–nanocomposite containing 3 wt % SiO_2.

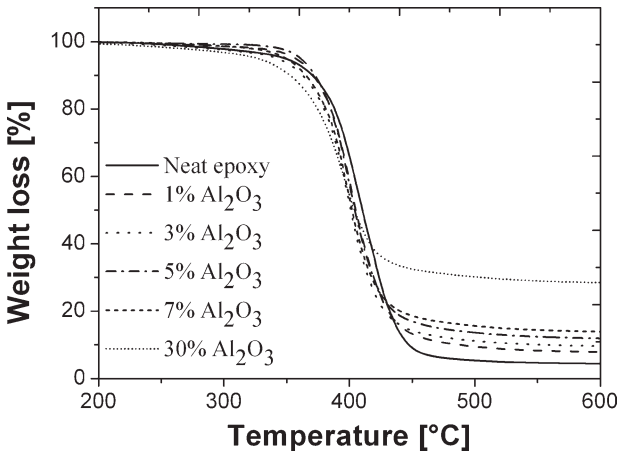

Figure 7 TGA curves of the epoxy resin and its nanocomposite containing Al_2O_3 filler.

modulus from the value of about 2.7 GPa, observed for the neat resin, to the value of about 3.2 GPa for the composite containing 3% Al_2O_3. When the filler content increased up to 30 wt %, a further improvement of the elastic modulus was observed (∼ 3.9 GPa). The elastic moduli of the nanocomposites were higher than those of neat epoxy resin in the whole temperature range between 0 and 130°C (see Fig. 8).

The peak position of the tan δ curves could be regarded as the glass-transition temperature (T_g) of the epoxy–nanocomposites. The tan δ peak area decreased and became broader with increasing nanofiller content; this indicated that the chain mobility of the crosslinked epoxy was restricted by the presence of nano-Al_2O_3 (Fig. 9). This resulted in an increase of the T_g values from 139°C for neat epoxy to 146°C for the composites with 3% Al_2O_3.

The effects of different ceramic nanofillers and relative amounts on E', evaluated at 25°C, and on T_g of the epoxy–nanocomposites are reported in Table III. As can be noticed, E' increased with filler content up to 3 wt %, reaching the maximum value of about 3.25 GPa for the composites containing 3% TiO_2. Also, the T_g values, reported in Table III, improved

TABLE II
Thermal Stability of the Epoxy–Nanocomposites at Different Filler Contents

wt %	T_{id} (3% weight loss; °C)
Neat epoxy	318
1% Al_2O_3	343
3% Al_2O_3	314
5% Al_2O_3	352
7% Al_2O_3	335
30% Al_2O_3	293
1% SiO_2	310
3% SiO_2	266
1% TiO_2	304
3% TiO_2	323

T_{id} = initial decompostition temperature.

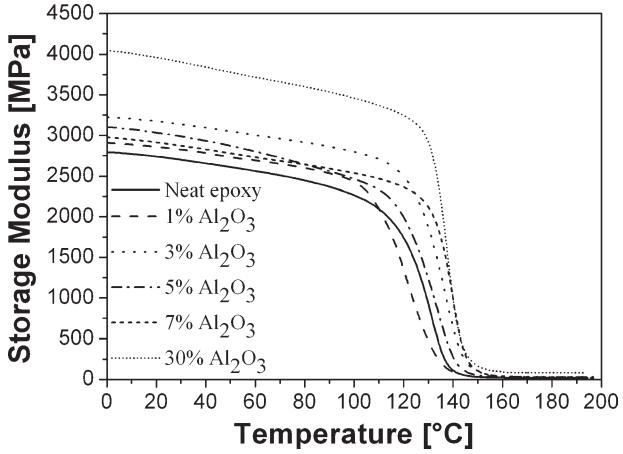

Figure 8 E' curves of the epoxy/Al_2O_3 nanocomposites.

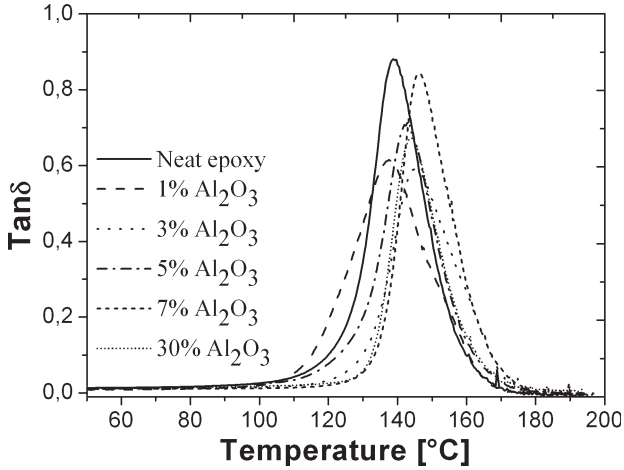

Figure 9 Tan δ curves of the epoxy/Al_2O_3 nanocomposites.

with the addition of all nanofillers up to 3 wt %. The addition of rigid nanoparticles with a very large surface area and the formation of the interface boundary region between the matrix and solid particles reduced the polymer chain mobility and resulted in increased T_g values for all of the composites. A slight decrease was ascertained when the filler content reached 7 wt %. This phenomena might have resulted from an uncompleted curing reaction between DGEBA and MTHPA because too many nanoparticles were added to the epoxy resin during the formation of the nanocomposites, which reduced their crosslinking density.[11]

Thermal conductivity (λ)

Thermal conductivity (λ) is a measure of the ease with which the temperature is transmitted through a material and is an important material property. The λ values of the neat epoxy and its various hybrids were evaluated by MDSC, according to ASTM E 1952.

Figure 10 shows the λ values for the epoxy–nanocomposites. The λ value for the 30% Al_2O_3–epoxy–nanocomposite is listed in Table IV, together the other values of all of the nanocomposites. The data are the average value of three measurements.

The highest λ values were obtained for Al_2O_3–epoxy samples at each filler loading because Al_2O_3 was the most thermally conductive filler (λ ≈ 40 W/mK) among the chosen fillers.

At lower filler contents, λ remained approximately constant for all specimens containing different fillers. When the Al_2O_3 content increased up to 30 wt %, the λ value was roughly doubled compared to the neat resin. This improvement, from 0.19 W/mK for the neat resin to 0.29 W/mK for the 30% Al_2O_3 sample, was due to the formation of a percolative pathway for heat conduction. In fact, the mode of thermal conduction in the amorphous polymer was mainly due to the presence of conductive paths formed by conductive particles, and factors that influenced λ could have been the size, amount, and shape of the particles.

TiO_2 and SiO_2 nanoparticles exhibited λ values lower than the Al_2O_3 one. Hence, the addition of low ceramic filler content did not affect the λ of the composites compared with the epoxy resin. A slight decrease of λ could be observed in the case of SiO_2 nanoparticles, probably because of the poor nanoparticle/matrix interface. In a similar way, λ decreased with filler content for the TiO_2 nanocomposites.

TABLE III
E' and T_g Values of Epoxy Neat Resin and Its Nanocomposites at Different Filler Contents

	Al_2O_3		TiO_2		SiO_2	
wt %	E' (GPa)	T_g (°C)	E' (GPa)	T_g (°C)	E' (GPa)	T_g (°C)
0	2.7	139	2.7	139	2.7	139
1	2.8	138	2.9	141	2.8	145
3	3.2	146	3.2	145	2.9	147
5	3.0	143	3.1	144	3.2	142
7	2.9	144	3.1	143	3.0	141
30	3.9	144	—	—	—	—

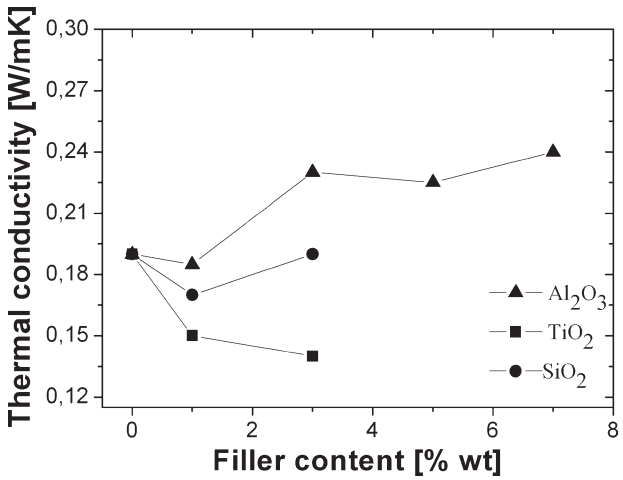

Figure 10 λ values of the epoxy–nanocomposites.

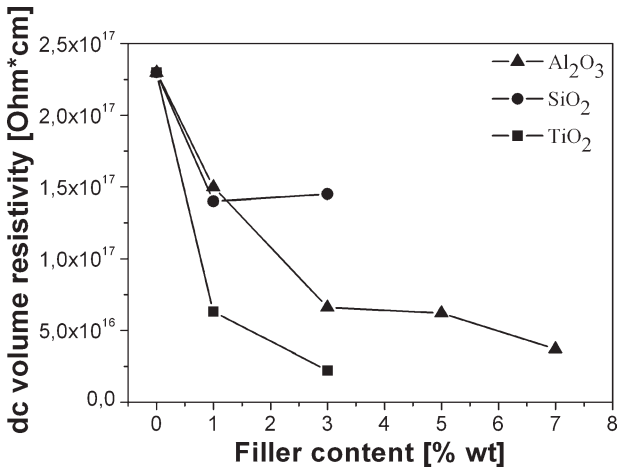

Figure 11 ρ_v of the epoxy–nanocomposites.

Volume resistivity (ρ_v)

Plane, disc-shaped samples characterized by a thickness ranging between 0.6 and 0.8 mm were prepared for electrical characterization. The volume resistivity was at 23°C, as we measured by holding the specimens in a suitably shielded cell and with a stabilized dc source and a picoammeter (HP 4140B) (Palo Alto, CA). Before the measurement, the specimens were held in an oven at the controlled temperature of 30°C for 48 h. ρ_v was measured by application of a dc voltage of 1400 V across the samples; this corresponded to an applied electrical field included in the interval from 15.5 to 23.0 kV/cm. The values of the electric current intensity were recorded after 120 s from the application of the dc voltage, when a stable state was reached. The data presented in this article are an average value of five samples. In Figure 11, the dc ρ_v versus the filler content (weight percentage) is reported for the three different typologies of samples. It can be noted a decrease of ρ_v with respect to the pure epoxy resin, which was more evident in the TiO_2 samples (in the 3 wt % samples, the resistivity was one order of magnitude lower with respect to the pure epoxy resin). Table V reports ρ_v values for all of the nanocomposites.

Dielectric parameters

ε_r and tg δ were measured at High Voltage (1.2 kV) and 50 Hz, at room temperature (23°C), by means of a dielectric test cell Tettex 2914 and a Haefely bridge type 470. The test cell is equipped with a flat heatable high-voltage electrode and with a shielded measuring electrode (guard ring) which eliminates partial capacitances which influence the test results. This type of test were performed to receive indications about the behavior of the insulating material when subjected to high electrical stresses at industrial frequency. In particular the presence of losses due to partial discharge activity can be identified by comparing the values of tg δ with those measured in low voltage tests. Results obtained as a function of the filler content, are reported in Table VI. As could be observed when the filler loading was increased, there was a decrease of ε_r values. The reduction was more evident in the TiO_2 samples, which at 3% filler content, exhibit $\varepsilon_r \approx 2.5$, which was much lower than the ε_r value of the neat epoxy resin ($\varepsilon_r \sim 3.1$). With regard to the tg δ, in all cases, a slight increase could be observed with the higher loading percentages: at 3 wt %, the Al_2O_3 composites showed the highest value (tg $\delta \sim 0.018$). The enhancement of tg δ could be associated with a sort of dc conduction mechanism, which was activated with increasing filler content.

TABLE IV
λ Values of Epoxy–Nanocomposites at Different Filler Contents

wt %	Al_2O_3	TiO_2	SiO_2
0	0.19	0.19	0.19
1	0.18	0.15	0.17
3	0.23	0.14	0.19
5	0.22	—	—
7	0.24	—	—
30	0.29	—	—

TABLE V
ρ_v of Epoxy–Nanocomposites at Different Filler Contents

wt %	Al_2O_3	TiO_2	SiO_2
0	2.3×10^{17}	2.3×10^{17}	2.3×10^{17}
1	1.5×10^{17}	6.3×10^{16}	1.4×10^{17}
3	6.6×10^{16}	2.2×10^{16}	1.6×10^{17}
5	6.2×10^{16}	—	—
7	3.7×10^{16}	—	—
30	7.4×10^{16}	—	—

TABLE VI
ϵ_r and Tan δ Values of the Epoxy–Nanocomposites at Different Filler Contents

	Al_2O_3		TiO_2		SiO_2	
wt %	ε_r	tg δ	ε_r	tg δ	ε_r	tg δ
0	3.1	0.007	3.1	0.007	3.1	0.007
1	2.9	0.011	2.9	0.011	2.7	0.012
3	2.7	0.018	2.5	0.008	2.8	0.010
5	2.8	0.011		—		
7	2.3	0.013				
30	3.3	0.010				

Dielectric spectroscopy

An insight into the way in which the included nanoparticles could affect the dielectric properties of materials could be obtained by dielectric spectroscopy. ε_r and tg δ of the epoxy–nanocomposites were measured at a low voltage (1.1 V) over a wide range of frequencies (10^2–10^6 Hz) with an impedance analyzer (HP 4192A) (Palo Alto, CA) and a suitable test cell (Agilent 16451B) (Mechelen Belgium). The dielectric test fixture was equipped with a four-terminal pair cable assembly and was used in the guarded electrode configuration.

During all of the measurements, the temperature was maintained at room values. Thus, the influence of the temperature on the results could be ignored. Figures 12 and 13 show the variations of the dielectric permittivity and tan δ as a function of frequency for Al_2O_3 epoxy composites.

ε_r of the epoxy–nanocomposites was governed by the polarization associated with the epoxy and nano-Al_2O_3 particles and the interfacial polarization at the interface between the epoxy and nanoparticles.[12] It is also well known that the frequency of the measurements will influence the polarization process. Thus as expected, it can be seen from Figure 12 that the epoxy–nanocomposites and unfilled epoxy showed a decrease in ε_r with increasing frequency. In a typical epoxy resin system, the permittivity of epoxy is determined by the number of orientable dipoles present in the system and their ability to orient under an applied electric field.[13,14] As in the epoxy chain, most of the free dipolar functional groups were able to orient under a lower frequency of applied field. Thus, the epoxy composites tended to have a higher permittivity in a lower frequency range. When the frequency of the applied voltage increased, it became more difficult for larger dipolar groups to orient themselves. Thus, the effect of dipolar groups on the permittivity was decreasing continuously as the frequency increased. Moreover, the increasing of frequency of the applied field also resulted in a reduction of the Al_2O_3 fillers' ε_r.[15] The combination of both effects resulted in the reduction of the epoxy–nanocomposites' permittivity with increasing frequency. It also can be seen from Figures 12 that ε_r for the nanocomposites decreased as the Al_2O_3 content increased and reached its lowest value when the loading content was more than 3 wt %. A reduction of ε_r with increasing Al_2O_3 content may have been caused by the interaction between the nanoparticles and the epoxy chain that reduced the mobility of the epoxy chain in the bulk material, which resulted in a decrease in the effective permittivity of the epoxy–nanocomposites.[16] When a small amount of nanofiller was loaded into epoxy, because of the interaction between the filler and epoxy chain, the thin immobile nanolayers could be formed. Those thin immobile nanolayers restricted the mobility of the epoxy chain.[17] As the loading concentration increased, more immobile nanolayer formed, and the mobility of epoxy chain decreased continuously; this resulted in a decrease of the nanocomposites' permittivity. A similar ε_r behavior was observed for the SiO_2 and TiO_2 nanocomposites.

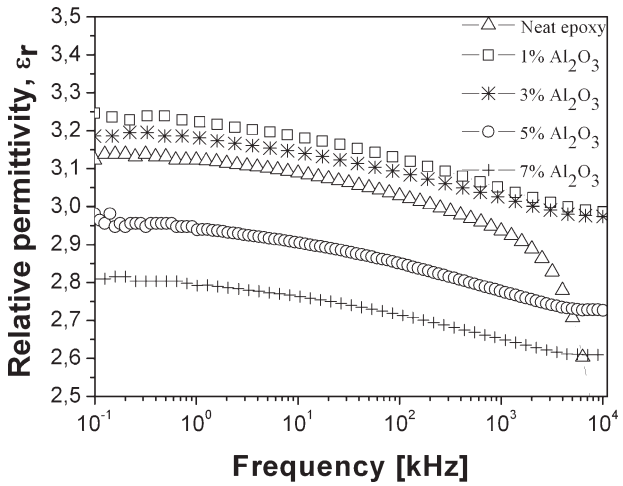

Figure 12 Frequency dependence of ε_r of the Al_2O_3–epoxy–nanocomposites.

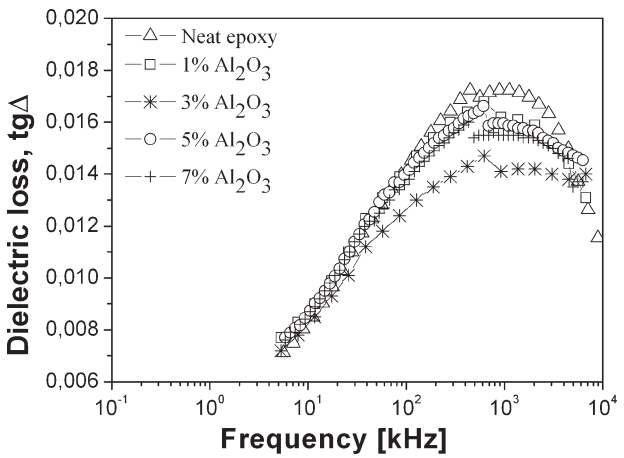

Figure 13 Frequency dependence of tan δ of the Al_2O_3–epoxy–nanocomposites.

tg δ dependence on the frequency is shown in Figures 13 for Al_2O_3–epoxy–nanocomposites: the tg δ values depend on the electrical conductivity.[18] The electrical conductivity, in turn, depended on the number of charge carriers in the bulk of the material, the relaxation time of the charge carriers, and the frequency of the applied electric field. The tg δ values marginally increased with frequency with the occurrence of a peak around 10^3 kHz and then slowly started to decrease. Corresponding to this behavior, the permittivity characteristics showed a marginal steep slope in the same frequency region at which the tg δ peak was observed. tg δ decreased with increasing frequency because the mobility of charge carriers was inhibited; this caused a reduction in the electrical conductivity through the volume of the material. In a polymeric system, such a process can occur due to hindrances in the charge transport mechanisms caused by defects and charge transport through different chains and interfaces.

CONCLUSIONS

In this article, epoxy–nanocomposites containing ceramic fillers were prepared by a combined dispersion technique, namely, mechanical mixing and sonication, followed by a step thermal curing process. SEM results revealed that there was a good filler dispersion. Different filler contents did not affect the degradation phenomena for the epoxy–nanocomposites compared with neat epoxy resin. It was found that both elastic modulus and T_g increased for all of the nanocomposites compared with neat resin.

At low filler contents (1 and 3 wt %), the threshold of continuous pathway is not reached and λ values are not significantly affected by the presence of particles. At high filler contents (30 wt %), the formation of a percolative heat sink pathway increased λ.

A slight reduction in the epoxy ρ_v was observed by the incorporation of a small amount of nanofiller into epoxy matrix.

The ε_r values at 50 Hz in the nanocomposites were found to be lower than that of neat epoxy resin; instead, the tg δ values were marginally increased compared with the epoxy matrix.

Dielectric spectroscopy study revealed a decrease in ε_r with increasing frequency both for unfilled epoxy resin and epoxy–nanocomposites. This behavior was due to inability of dipolar groups to orient themselves when the frequency of the applied voltage increases. As concern as tg δ values, they slightly increased with increasing frequency with the occurrence of a peak around 10^3 kHz and then slowly start to decrease.

References

1. Omrani, A.; Simon, L. C.; Rostami, A. A. Mater Chem Phys 2009, 114, 145.
2. Lee, G.; Park, M.; Kim, J.; Lee, J. I.; Yoon, H. Compos A 2006, 37, 727.
3. Fan, L.; Su, B.; Qu, J.; Wong, C. P. Int Symp Adv Packaging Mater 2004, 9, 193.
4. Han, Z.; Wood, J. W.; Herman, H.; Zhang, C.; Stevens, G. C. IEEE Trans Dielectr Electr Insul 2008, 497.
5. Singha, S.; Thomas, M. J. IEEE Trans Dielectr Electr Insul 2008, 15, 12.
6. Kochetov, R.; Andritsch, T.; Lafont, U.; Morshuis, P. H. F.; Smit, J. J. Annu Rep Conf Electr Insul Dielectr Phenom 2009, 658.
7. Kochetov, R.; Andritsch, T.; Lafont, U.; Morshuis, P. H. F.; Smit, J. J. Annu Rep Conf Electr Insul Dielectr Phenom 2009, 523.
8. Maity, P.; Poovamma, P. K.; Bassu, S.; Parameswaran, V.; Gupta, N. IEEE Trans Dielectr Electr Insul 2009, 16, 1481.
9. Kim, S. W.; Choi, B.; Lee, S. H.; Kang, K. H. High Temp–High Pressure (8th Asian Thermophys Properties Conf) 2007, 37, 21.
10. Lekakou, C.; Murugesh, A. K.; Smith, P. A. Polym Eng Sci 2008, 216.
11. Chen, C.; Jian, J.; Yen, F. Compos A 2009, 40, 463.
12. Wang, Q.; Chen, G.; Alghamdi, A. S. Int Conf Solid Dielectr 2010, 1.
13. Eloundou, J. P. Eur Polym J 2002, 38, 431.
14. Zhang, L. D.; Zhang, H. F.; Wang, G. Z.; Mo, C. M.; Zhang, Y Phys Status Solidi 1996, 157, 483.
15. Nelson, J. K.; Fothergill, J. C. Nanotechnology 2004, 15, 586.
16. Shi, H.; Gao, N.; Jin, H.; Zhang, G.; Peng, Z. IEEE 9th Int Conf Properties Appl Dielectr Mater 2009, 804.
17. Tsagaropoulos, G.; Eisenberg, A. Macromolecules 1995, 28, 6067.
18. Singha, S.; Thomas, M. J. IEEE Trans Dielectr Electr Insul 2009, 1.